Development 136, 563-574 (2009) doi:10.1242/dev.016816

The cell migration molecule UNC-53/NAV2 is linked to the ARP2/3 complex by ABI-1

Kristopher L. Schmidt[1,2], Nancy Marcus-Gueret[1,2], Adetayo Adeleye[1,2], Jordan Webber[1], David Baillie[2] and Eve G. Stringham[1,2,*]

The shape changes that are required to position a cell to migrate or grow out in a particular direction involve a coordinated reorganization of the actin cytoskeleton. Although it is known that the ARP2/3 complex nucleates actin filament assembly, exactly how the information from guidance cues is integrated to elicit ARP2/3-mediated remodeling during outgrowth remains vague. Previous studies have shown that *C. elegans* UNC-53 and its vertebrate homolog NAV (Neuronal Navigators) are required for the migration of cells and neuronal processes. We have identified ABI-1 as a novel molecular partner of UNC-53/NAV2 and have found that a restricted calponin homology (CH) domain of UNC-53 is sufficient to bind ABI-1. ABI-1 and UNC-53 have an overlapping expression pattern, and display similar cell migration phenotypes in the excretory cell, and in mechanosensory and motoneurons. Migration defects were also observed after RNAi of proteins known to function with *abi-1* in actin dynamics, including *nck-1*, *wve-1* and *arx-2*. We propose that UNC-53/NAV2, through its CH domain, acts as a scaffold that links ABI-1 to the ARP2/3 complex to regulate actin cytoskeleton remodeling.

KEY WORDS: Cell migration, Axonal guidance, Cytoskeleton, ARP2/3 complex, *C. elegans*

INTRODUCTION

The successful development of multicellular organisms requires that cells and cellular processes migrate sometimes long distances to well-defined target locations. To achieve such a journey, the cell must repeatedly reorganize its cytoskeleton in response to a multitude of navigational cues. The nematode *Caenorhabditis elegans* has proven to be an excellent model organism for the elucidation of global guidance mechanisms controlling migration. Several signals and receptors reported to control cell migration in vertebrates have been described in *C. elegans*, including: UNC-6/netrin and its receptors UNC-40/DCC and UNC-5 (Hedgecock et al., 1990; Ishii et al., 1992), the SLT-1/SLIT cue (Hao et al., 2001) and its multifunctional receptor SAX-3/ROBO (Ghenea et al., 2005; Levy-Strumpf and Culotti, 2007; Zallen et al., 1998), WNTs and their associated FZ receptors (Pan et al., 2006), and growth factors such as EGL-17/FGF (Burdine et al., 1997) and its receptor EGL-15/FGFR (Birnbaum et al., 2005; Bulow et al., 2004; DeVore et al., 1995). Besides the identification of the signaling cues and their receptors, the machinery required for the subcellular positioning of receptors is also being uncovered. For example, recent evidence suggests that the kinesin-like molecule VAB-8 localizes SAX-3/ROBO to the cell surface to modulate the response to SLT-1 guidance cues (Watari-Goshima et al., 2007), and that both MIG-2/RhoGTPase and VAB-8 are required for the localization of the UNC-40 receptor (Levy-Strumpf and Culotti, 2007).

At the leading edge of motile cells, local reorganization of the actin cytoskeleton is mediated by the ARP2/3 complex, which nucleates the assembly of branched actin filaments (Higgs and Pollard, 2000; Volkmann et al., 2001). Potential regulators of ARP2/3 include the ABI proteins, initially discovered to function as downstream targets of ABL non-receptor tyrosine kinases implicated in RAC-dependent cytoskeletal organization and remodeling (Courtney et al., 2000; Funato et al., 2004; Jenei et al., 2005; Stradal et al., 2001), in addition to processes such as cell migration, neuronal development, growth cone pathfinding and endocytosis (Courtney et al., 2000; Grove et al., 2004; Ibarra et al., 2005; So et al., 2000). ABI family members localize to the actin-rich tips of lamellipodia and filopodia, and are widely expressed in the developing murine nervous system (Courtney et al., 2000; Stradal et al., 2001). ABI forms part of the pentameric WAVE complex together with NAP-1, PIR121/SRA-1, HSPC300 and WAVE, which has been shown to mediate actin remodeling through ARP2/3 (Bompard and Caron, 2004; Takenawa and Suetsugu, 2007). The WAVE complex members WVE-1, GEX-2 (SRA-1) and GEX-3 (NAP-1) have been characterized in *C. elegans*. GEX-2 and GEX-3 colocalize to cell boundaries during embryogenesis and interact physically (Soto et al., 2002), and loss of WVE-1 or the GEXs results in defective hypodermal cell migration, incomplete ventral enclosure during morphogenesis, and embryonic lethality (Soto et al., 2002; Withee et al., 2004). Additionally, ventral enclosure defects in WVE-1 and GEX mutants are reminiscent of those found in RAC and ARP2/3 mutant animals, suggesting that a conserved pathway involving RAC, the WAVE complex and ARP2/3 is maintained during embryogenesis in *C. elegans* (Sawa and Takenawa, 2006; Soto et al., 2002; Withee et al., 2004).

While much has been uncovered with respect to the signaling events at the cell surface and the mechanics of actin filament assembly, relatively little is known about the proteins that integrate guidance information to instruct cytoskeletal reorganization. One candidate is UNC-53, initially discovered to control the migration of a subset of cells and cellular extensions along the anterior to posterior axis in *C. elegans*. Hypomorphic alleles of *unc-53* display reduced extension and guidance defects in the outgrowth of the mechanosensory neurons (Hekimi and Kershaw, 1993), the excretory canals (Hedgecock et al., 1990; Stringham et al., 2002) and the sex muscles, the latter resulting in an egg-laying defective phenotype in hermaphrodites (Stringham et al., 2002). By contrast,

[1]Department of Biology, Trinity Western University, 7600 Glover Road, Langley, BC V2Y 1Y1, Canada. [2]Department of Molecular Biology and Biochemistry, 8888 University Drive, Simon Fraser University, Burnaby, BC V5A 1S6, Canada.

*Author for correspondence (e-mail: stringha@twu.ca)

Accepted 9 December 2008

overexpression of UNC-53 in muscle cells results in exaggerated outgrowth during embryogenesis (Stringham et al., 2002). UNC-53 interacts genetically and physically with the SH2-SH3 adaptor protein SEM-5 (GRB-2), a mediator of EGL-15/FGFR signaling in sex myoblast migration in *C. elegans* (Chen et al., 1997; Stringham et al., 2002), suggesting a role for UNC-53 in signal transduction. UNC-53 also contains several domains observed in actin-binding proteins, suggesting a possible function in actin cytoskeleton dynamics (Stringham et al., 2002).

Roles in cell migration have also been documented for the vertebrate homologs of UNC-53. Three human UNC-53 homologs (NAV1, NAV2 and NAV3; Neuron Navigator 1, 2 and 3) have been identified (Maes et al., 2002; Merrill et al., 2002). The most similar homolog to UNC-53, NAV2, is retinoic acid inducible in the developing nervous system (Merrill et al., 2002), and hypomorphic mice have sensory deficits subsequent to morphological defects that are consistent with a role for NAV2 in neuron outgrowth (Peeters et al., 2004). NAV1 associates with microtubule plus-ends on developing neuronal growth cones and is required for netrin-induced directionality in pontine neurons (Martinez-Lopez et al., 2005). The NAV proteins are also expressed in a range of adult tissues, including brain, heart and kidney, in both mice and humans following outgrowth (Maes et al., 2002; Martinez-Lopez et al., 2005; Peeters et al., 2004), and *Nav3* mRNA is localized to synapses at neuromuscular junctions (Kishi et al., 2005).

In this study, we show that the largest UNC-53 isoforms are expressed in several migrating cells in which UNC-53 is required, as well as in adult cells. Additionally, we show that UNC-53 binds the *C. elegans* ABI-1 homolog, and that loss of ABI-1 leads to migration defects similar to those found when *unc-53*, *wve-1*, *nck-1* and *arx-2* (*arp2*) are removed. We find that UNC-53 and ABI-1 have an overlapping pattern of expression, and that disruption of the interaction between UNC-53 and ABI-1 impairs longitudinal guidance. Finally, we propose a model for how UNC-53 might function with ABI-1 and the ARP2/3 complex in cytoskeletal remodeling.

MATERIALS AND METHODS

C. elegans strains

C. elegans Bristol (N2) and mutant strains were maintained according to standard protocols (Brenner, 1974). Strains used in this study include:

BC06288 *ppgp12::gfp (sIs10089)*;

ZB171 *pmec-4::gfp (bzIs7)*;

BC12924 *pnck-1::gfp (sIs12798* [*dpy-5(e907)*/*dpy-5(e907)*; sEx12728 [rCesZK470.5::GFP + pCeh361]*)*;

BC14371 *punc-53L::gfp (sEx14371* [*dpy-5(e907)*/*dpy-5(e907)*; sEx14371 [rCesF45E10.1a::GFP + pCeh361]*)*;

BC10129 *pabi-1::gfp (sEx10129* [*dpy-5(e907)*/*dpy-5(e907)*; sEx14371 [rCesB0336.6::GFP + pCeh361]*)*;

VA97 *pabi-1::abi-1::gfp (pmEx97* [pabi-1::abi-1(1-1410)::GFP + pRF4]*)*;

VA71 *unc-53(n166); sIs10089*;

VA106 *unc-53(n152); sIs10089*;

VA72 *unc-53(n166); bzIs7*;

FX494 *abi-1(tm494)* (684bp deletion III: 5690340…5691023);

VA74 *abi-1(tm494); sIs10089*;

VA99 *abl-1(ok171); sIs10089*;

VA100 *wsp-1(gm324); sIs10089*;

VA75 *abi-1(tm494); bzIs7*;

VA76 *nck-1(ok694)*; *sIs10089* [*nck-1(ok694)* contains a 1814bp deletion X: 4150378…4152191];

VA77 *nck-1(ok694); bzIs7*;

VA79 *unc-53(n166); abi-1(tm494); sIs10089*;

VA91-VA92 *abi-1(tm494)*; *sIs10089*; *pmEx91-92* [ppgp12::abi-1(1-1410) + pDPY-30::NLS::DSRED2 (Cordes et al., 2006)];

VA93-VA96 *sIs10089; pmEx93-96* [ppgp12::unc-53(1-416)::GFP + pDPY-30::NLS::DSRED2 (Cordes et al., 2006)];

VA103-VA104 *unc-53(n152); sIs10089; pmEx103-104* [ppgp12::unc-53(1-4965) + pDPY-30::NLS::DSRED2 (Cordes et al., 2006)];

VH715 *nre-1(hd20); lin-15b(hd126); hdIs17; hdIs10*; and

VA78 *eri-1(mg366); bzIs7*.

Yeast two-hybrid assays

A *Nde*I-*Nco*I fragment of the *unc-53* cDNA (nucleotides 64-480 corresponding to amino acids 1 to 139) was subcloned into pAS2 (Matchmaker, Clontech Laboratories) to generate pVA200. Using pVA200 as bait and a mixed stage *C. elegans* cDNA library as prey (gift of Bob Barstead, Oklahoma Medical Research Foundation, Oklahoma, USA) candidate binding partners were identified in a yeast two-hybrid screen by assaying for growth on triple drop-out media (–Trp-Leu-His) and the β-galactosidase activity of doubly transformed yeast Y190 cells as described (Aspenstrom and Olson, 1995). Six of the positives corresponded to the B0336.6/*abi-1* locus. pVA305 corresponds to the shortest *abi-1* cDNA isolated in the screen cloned into the pSE1107 vector, coding for amino acids 12 to 427 of ABI-1, and was used for subsequent biochemical studies.

In vitro binding assays

ABI-1::GST and UNC-53N::6×His protein were purified from BL21(DE3) *E. coli* harboring pVA600 and pVA63, respectively. pVA600 was generated by inserting a 1.3-kb *Xho*I fragment from pVA305 into pGEX4T2 (Invitrogen). Recombinant proteins ABI-1::GST or GST were expressed and purified according to the manufacturer's instructions (Invitrogen), with modifications (Frangioni and Neel, 1993). Ten micrograms of ABI-1::GST or GST were applied to glutathione resin for pull-down experiments. Total UNC-53N::6×His lysates (25 μg) were applied to ABI-1::GST or GST glutathione resin and incubated at 4°C for 3 hours. Following incubation, beads were washed four times with 20 mM Tris pH 7.4, 0.1 mM EDTA, 300 mM NaCl and 0.1% Triton X-100, and bound proteins were extracted and analyzed by SDS-PAGE and western blotting.

RNA interference and mutant analysis

RNAi experiments were performed by feeding (Kamath et al., 2001), using RNAi clones obtained from Geneservice, with the exception of the *unc-53L* RNAi clone pVA504, which was generated by cloning a 0.3-kb *Xho*I-*Nco*I PCR fragment corresponding to nucleotides 1 to 280 (exons 1-4) of the *unc-53* cDNA from pTB113 (Stringham et al., 2002) in tandem into pPD129.36 (gift of Andrew Fire, Stanford University School of Medicine, Stanford, USA). Animals carrying the *ppgp-12::gfp* reporter were scored for excretory canal outgrowth with respect to the position of the gonad arms, the vulva and the anus. Neuronal RNAi was carried out using either the neuronal enhanced sensitive strain *eri-1(mg366); pmec-4::gfp* for mechanosensory neurons (Kennedy et al., 2004), or *nre-1(hd20); lin15b(hd126)* for motoneurons. The anterior process of the PLM neuron was scored as abnormal if the stop point was posterior to the wild-type position at the mid-body. Ventral cord motoneurons commissures were determined to have defects if two or more axons exhibited ectopic lateral branching or stalling and were unable to reach the dorsal cord.

Preparation of UNC-53 and ABI-1 polyclonal antisera

A *Sac*I-*Nco*I fragment of the *unc-53* cDNA (nucleotides 64-480) that corresponds to amino acids 1 to 139 was subcloned into the expression vector pRSET (Amersham Pharmacia) to generate pVA63, which was then expressed in *E. coli* BL21 cells according to manufacturer's protocols (Invitrogen). Purified protein was emulsified in Titre Max Gold and injected into a female New Zealand white rabbit. The antiserum collected was active at titers of 1:30,000 on western blots of recombinant fusion protein. The specificity of *PAb-UNC-53N* was confirmed by staining animals that ectopically express UNC-53 in the intestine under control of the *hsp-16* promoter (Stringham et al., 1992). Whereas no staining was observed in control animals, strong staining in the cytoplasm of intestinal cells was observed after heat shock. For the generation of ABI-1 polyclonal antibody (*PAb-ABI-1*), a synthesized peptide (DYNSIYQPDRYGTIRAGGR)

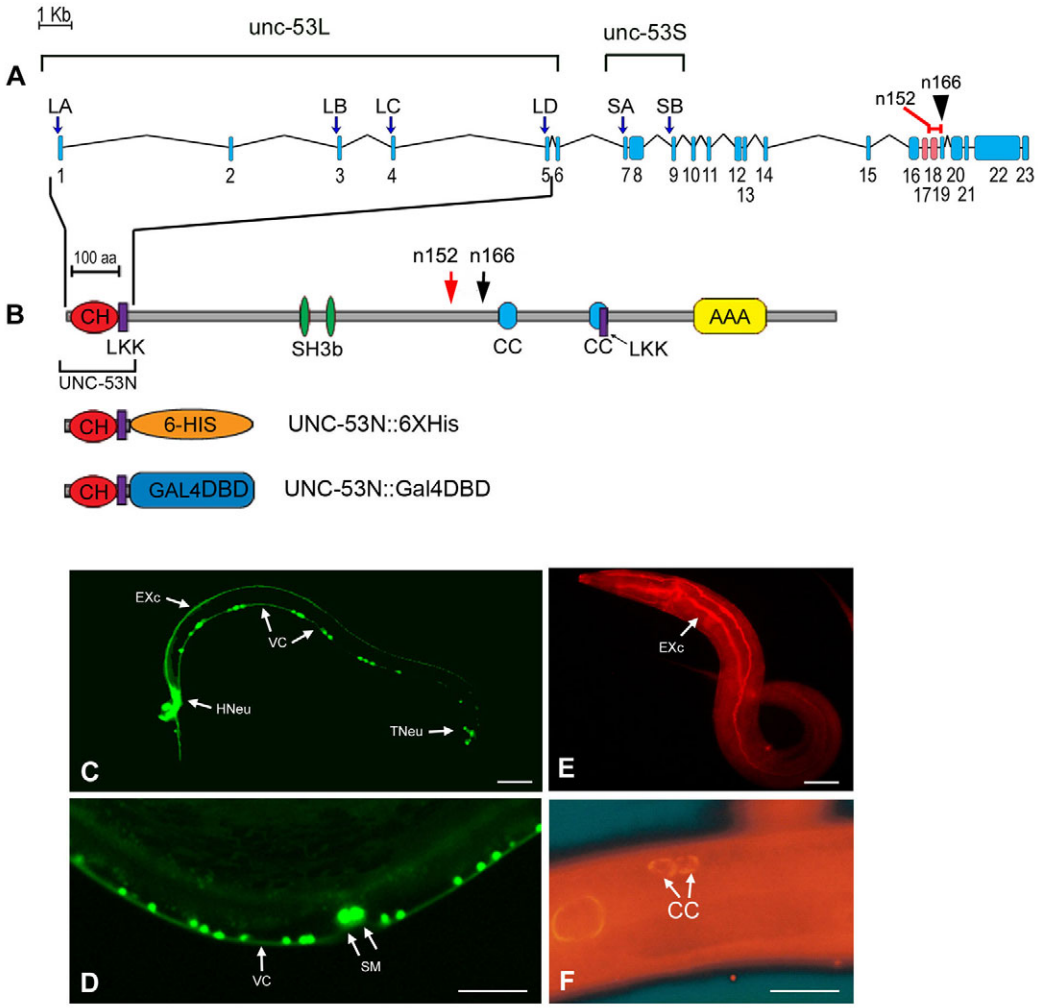

Fig. 1. Characterization of the long isoforms (UNC-53L) of *unc-53*. (**A**) Structure of the *unc-53* gene. The start of the various UNC-53L and UNC-53S isoforms are indicated by arrows. The promoter for UNC-53SA is between exons 5 and 8, and the promoter for UNC-53SB is located between exons 8 and 13 (Choi and Newman, 2006; Stringham et al., 2002). 2.9 kb of DNA upstream of the transcriptional start site of UNC-53LA was used to construct *punc-53L::gfp*. Alternatively spliced exons are shown in pink. *unc-53(n152)* is a 319-bp deletion removing parts of exons 18 and 19, producing a stop codon in exon 20 (Stringham et al., 2002), and *n166* is a single nucleotide C to T transition in exon 19 that introduces a premature stop codon. (**B**) The longest polypeptide, UNC-53LA, is 1654 amino acids and contains a calponin homology domain (CH, red; amino acids 11-109), two LKK motifs (LKK, purple; 114-133 and 1097-1116), two proline-rich SH3-binding motifs (SH3b, green; 487-495 and 537-545), two coiled-coil regions (CC, blue; 890-923 and 1078-1113) and an AAA domain (yellow; 1292-1425). *n166* introduces a premature stop codon at amino acid 949. Both *n152* and *n166* remove the coiled-coil, LKK and AAA domains from all isoforms. The first five exons of UNC-53 (UNC-53N; amino acids 1-139) were used for the production of PAB-UNC-53N antisera and the GAL4 DNA-binding domain (GAL4DBD) in pVA200 for yeast two-hybrid studies. (**C**,**D**) Expression pattern using *punc-53L::gfp*. (C) Adult hermaphrodite (anterior is left), showing GFP expression in head (HNeu) and tail (TNeu) neurons, the excretory cell (EXc), and the ventral nerve cord (VC). (D) Midbody, showing expression in the sex myoblasts (SM) and the ventral cord (VC). (**E**,**F**) Expression pattern using *PAb-UNC-53N* antisera. (E) Expression of UNC-53L throughout the excretory cell and canals (EXc). (F) UNC-53L expression in a pair of coelomocytes (CC). Scale bars: 100 μm.

containing amino acids 256-274 from ABI-1 was coupled to keyhole limpet hemocyanin (KLH) and used to immunize guinea pigs (Open Biosystems). Anti-sera were affinity purified towards the ABI-1 peptide and were active at a dilution of 1:10,000 on western blots of recombinant protein.

Expression pattern of UNC-53L and ABI-1

To detect UNC-53L and ABI-1 in vivo by immunostaining, staged larvae or adults were fixed and permeabilized according to the method of Ruvkun and Finney (Bettinger et al., 1996). *PAb-UNC-53N* was used at 1:500 dilution and *PAb-ABI-1* antibody at 1:100, with secondary anti-Rabbit IgG (Invitrogen Molecular Probes) and anti-Guinea Pig IgG (Open Biosystems) used at 1:500 and 1:400, respectively. Anti-GFP immunostaining was performed using chick anti-GFP primary at 1:100 with secondary rabbit anti-Chick IgG at 1:400 (Millipore, USA), directed towards the VA97 strain. VA97 contains the extrachromosomal array *pmEx97* generated by co-injecting 1 ng/μl of the *pabi-1::abi-1::gfp*, containing 0.5 kb upstream of *abi-1* and the entire *abi-1* locus fused to GFP with the pRF4 co-injection marker at 100 ng/μl. Expression of *abi-1* and *unc-53L* were also determined using promoter GFP transcriptional fusions. The *pabi-1::gfp* fusion (BC10129) included 275 bp upstream of *abi-1* fused to GFP, whereas 2.9 kb upstream of *unc-53* was fused to GFP to generate BC14371 (McKay et al., 2003). Specimens were viewed with Olympus IX81 or Leica DMLB fluorescence microscopes using appropriate filter sets.

Cell autonomy and overexpression experiments

Rescue of the *abi-1(tm494)* posterior canal defects was achieved by co-injecting 10 ng/μl of the PCR fusion *ppgp12::abi-1*, containing the *pgp-12* promoter (Zhao et al., 2005) fused to full-length *abi-1*, with 100 ng/μl of the

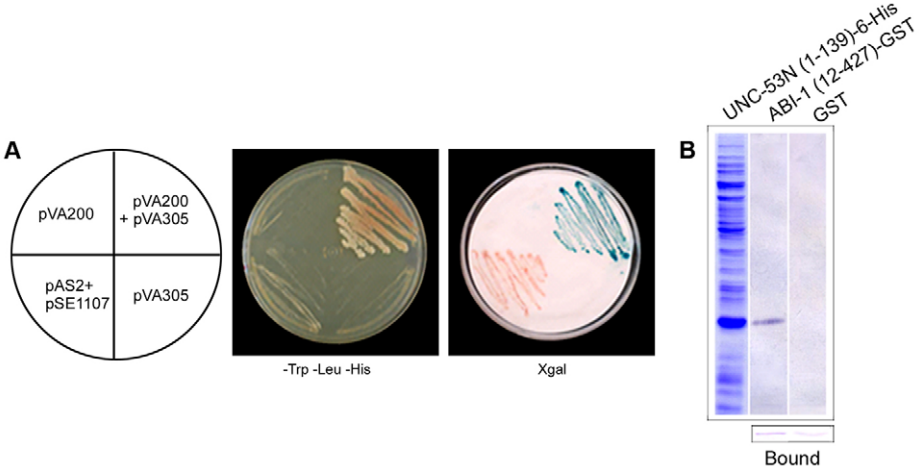

Fig. 2. ABI-1 physically interacts with the N terminus of UNC-53. (**A**) ABI-1::GAL4AD interacts with UNC-53N::GAL4DBD by yeast two-hybrid assay. Yeast harboring both bait (pVA200) and prey (pVA305) plasmids grow in triple drop-out media (–Trp-Leu-His) and are positive for β-galactosidase, in contrast to yeast transformed with empty vectors (pAS2 and pSE1107), or with either the bait or prey vector alone. (**B**) GST pull-down assay. Equal amounts of ABI-1(12-427)-GST and GST alone were expressed in *E. coli* and bound to glutathione-conjugated beads (Bound). Soluble UNC-53N::6His lysates (left lane) were incubated with protein-bound beads and were observed to bind ABI-1(12-427)-GST (middle lane) but not GST alone (right lane), as detected by *PAb-UNC-53N*.

plasmid pDPY-30::NLS::DSRED2 (Cordes et al., 2006) into the strain VA74 to create *vaEx91* and *vaEx92*. *unc-53(n152)* posterior canal defects were rescued by co-injecting the PCR fusion *ppgp12::unc-53L* (100 ng) with pDPY-30::NLS::DSRED2 into VA106 and scoring transgenic *unc-53(n152)* homozygous animals as described. UNC-53CH-expressing arrays *vaEx93-vaEx96* were generated by co-injecting *ppgp-12::unc-53CH::gfp* containing the *pgp-12* promoter fused to the first 422 nucleotides of *unc-53* cDNA from pVA63 and GFP at 100 ng/μl, along with 100 ng/μl of the plasmid pDPY-30::NLS::DSRED2 (Cordes et al., 2006) into the strain BC06288. Excretory canal morphology was scored in young adult animals co-expressing GFP and dsRED from all lines for general defects and for posterior canal migration position, as described above.

RESULTS

Characterization of UNC-53L

The *unc-53* locus is large, contains 23 exons, and encodes six polypeptides, the largest consisting of 1654 amino acids (Fig. 1A,B) (Stringham et al., 2002). Several protein motifs are shared between UNC-53 and its orthologs, including a calponin homology (CH) domain, two putative actin-binding sites of the LKK motif, two coiled-coil regions, two polyproline-rich SH3-binding motifs, and an AAA (ATPases associated with diverse cellular activities) domain (Stringham et al., 2002). A combination of alternative trans-splicing and cis-splicing events and the presence of two intronic promoters gives rise to four large isoforms of UNC-53 (LA, LB, LC and LD), collectively referred to as UNC-53L, and two small isoforms of UNC-53 (SA and SB), referred to as UNC-53S. Previous studies indicate that the intronic promoters that transcribe UNC-53SA and UNC-53SB have complementary non-overlapping expression patterns (Stringham et al., 2002). To characterize the expression of the UNC-53L isoforms, a promoter region 2.9-kb upstream of the most 5′ SL1 splice site of *unc-53* was used, and strong GFP expression was observed in the excretory cell, in neurons in head and tail ganglia, and in several classes of ventral cord motoneuron (Fig. 1C), as well as in the sex myoblasts (Fig. 1D). Immunostaining with an antibody raised against the translated product of the first 5 exons of *unc-53* (Fig. 1B) revealed UNC-53L protein localized in the cytoplasm of the excretory cell (Fig. 1E), the sex myoblasts, the anal muscles, the head neurons and the coelomocytes (Fig. 1F). Expression was detected at all developmental stages, including adults.

UNC-53L interacts with Abelson Interactor-1 (ABI-1)

Previous studies suggest that UNC-53 functions in signal transduction during migration (Stringham et al., 2002), yet few molecules known to interact directly with UNC-53 have been identified. Moreover, a phage cDNA devoid of the first four exons was sufficient to partially rescue the Unc and Egl phenotypes of *unc-53* mutants (Stringham et al., 2002). Therefore, we wondered what molecules might interact with the N-terminal of UNC-53, as this region is conserved in NAV2 and NAV3. To answer this question, we screened for interactors in a *C. elegans* yeast two-hybrid library, using the N terminus (UNC-53N) as bait (Fig. 1B). Of the candidates isolated, six corresponded to the B0336.6 genomic locus, the *C. elegans abi-1* (Abelson Interactor-1) homolog (Fig. 2A). Of the *abi-1* clones isolated, the smallest cDNA encoded amino acids 12-427, thereby excluding the SH3 region of ABI-1 as a required domain for UNC-53 binding. Moreover, the UNC-53 bait contained only the first 139 amino acids of UNC-53L, and thus was devoid of the polyproline repeats that are typical of SH3-binding domains. Therefore, the interaction between ABI-1 and UNC-53 does not appear to be mediated by SH3 binding. The yeast two-hybrid data was further confirmed by GST pull down (Fig. 2B), demonstrating that the interaction between ABI-1 and UNC-53 is direct.

Characterization of *abi-1*

BLAST analysis revealed the presence of a single *abi-1* gene in *C. elegans*. The *abi-1* genomic locus spans 2624 bp and contains five exons encoding a predicted polypeptide of 469 amino acids (Fig. 3). *C. elegans* ABI-1 is a conserved protein that is homologous to ABI-1 of *C. briggsae* (CAE64316), *Homo sapiens* (NP_005461), *Mus musculus* (Q3TJ64) and *Drosophila melanogaster* (NP_477263). The highest degree of homology resides within several recognizable protein domains suggestive of function. Near the N terminus is a Q-SNARE motif (Echarri et al., 2004), which in the case of mammalian ABI-1, has been shown to be involved in growth factor receptor endocytosis and to bind Syntaxin 1 (Echarri et al., 2004; Tanos and Pendergast, 2007). Partially overlapping with the Q-SNARE motif is an ABL-homeodomain homologous region that is similar to the DNA-binding region of homeodomain proteins, and which is found exclusively in adaptor proteins that interact with Abl-family tyrosine kinases (Dai and Pendergast, 1995). Additionally, *C. elegans* ABI-1 contains a serine-rich region and multiple polyproline-rich putative SH3-binding motifs. A single SH3 domain is located at the C terminus of *C. elegans* ABI-1 and this domain has been shown to mediate the interaction of ABI-1 with Abelson tyrosine kinases (Shi et al., 1995), and to control the ability of ABL to phosphorylate downstream targets, including mammalian enabled (Mena) (Tani et al., 2003). The *abi-1(tm494)* allele (Mitani Laboratory, National Bioresource Project) carries a 684-bp deletion

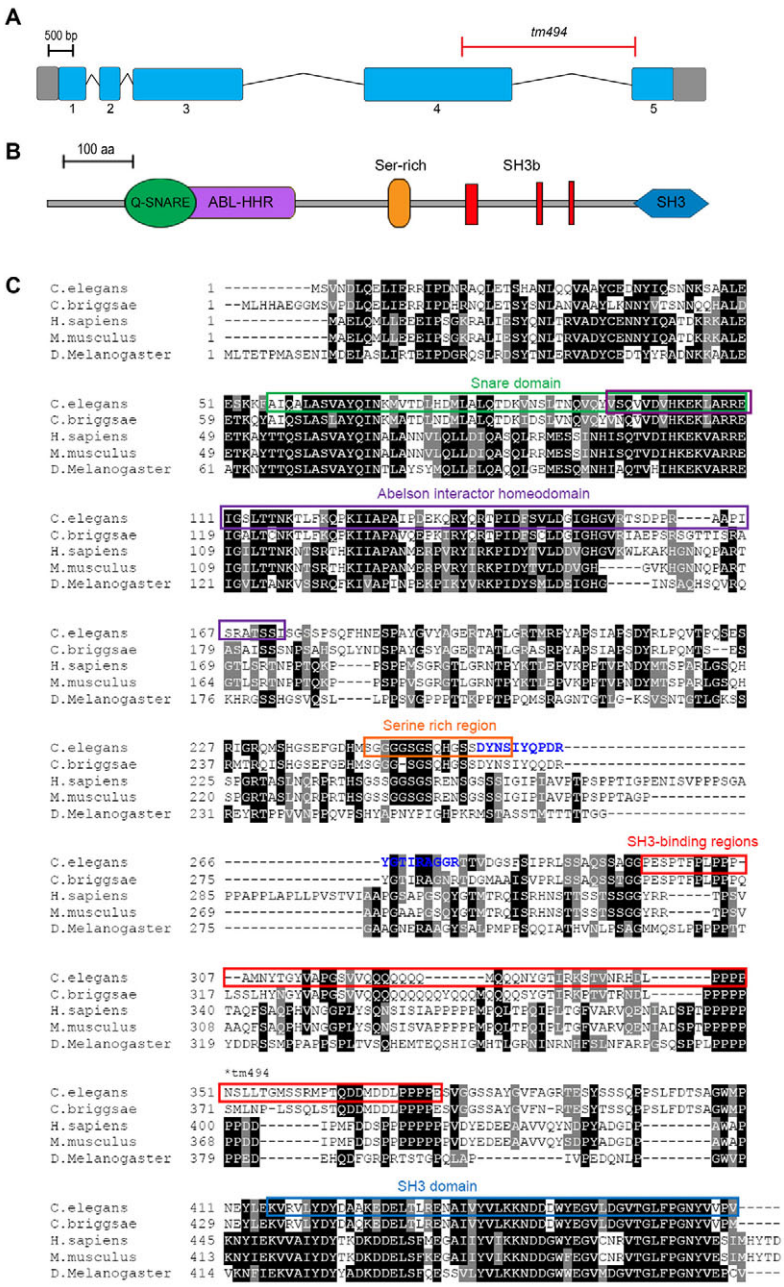

Fig. 3. Molecular organization of *C. elegans* ABI-1 gene and protein. (**A**) Gene structure of *abi-1*. The boundaries of introns, exons and the *abi-1(tm494)* deletion are indicated. (**B**) Protein structure of ABI-1. ABI-1 contains a Q-SNARE domain (Q-SNARE, green; amino acids 56-110) (Echarri et al., 2004), an Abl-interactor homeodomain homologous region (ABL-HHR, purple; 95-173), a serine-rich region (Ser-rich, orange; 243-259), three proline-rich SH3-binding motifs (SH3b, red; 296-306, 347-351 and 371-374) and an SH3 domain (SH3, blue; 416-469). ABL-HHR and SH3 domains were predicted using the Simple Modular Architecture Research Tool (SMART, http://smart.embl-heidelberg.de). (**C**) Comparison of *C. elegans* ABI-1 with *C. briggsae*, human, mouse and *Drosophila* orthologs. Multiple alignments were performed using Clustal W 1.83 (http://align.genome.jp) with ABI-1 proteins from *C. elegans* (CE29545), *C. briggsae* (CAE64316), *H. sapiens* (NP_005461), *M. musculus* (Q3TJ64) and *D. melanogaster* (NP_477263), and were drawn using BOXSHADE (http://www.ch.embnet.org). The peptide sequence used to generate ABI-1 antibody *PAb-ABI-1* is indicated in blue and the start site of the *tm494* deletion is indicated by an asterisk.

beginning at nucleotide 1659 in exon 4 (Fig. 3A), and encodes a predicted truncated product ending at proline 350 followed by TGPVRL and a premature stop codon, resulting in a 356 amino acid product (Fig. 3C).

Overlap in *unc-53* and *abi-1* mutant phenotypes

UNC-53 controls the migration of several cells and cellular processes along the anteroposterior axis in *C. elegans*, including the sex myoblasts (Chen et al., 1997), the ALN/PLN and ALM/PLM axons, and the excretory cell (Stringham et al., 2002). To determine whether the observed interaction between ABI-1 and UNC-53 is relevant in vivo, the migration phenotypes of *abi-1* were characterized. The migration and outgrowth of both the anterior and posterior excretory canal processes were visualized using the transgenic reporter *ppgp-12*::*gfp*, which is expressed exclusively in the excretory cell from the 3-fold embryonic stage onwards (Zhao et al., 2005). The excretory cell (EC) is a large H-shaped cell in *C. elegans* and represents an excellent cell type for the study of both dorsoventral and anteroposterior migrations. During its outgrowth, two processes emerge from the EC body and migrate dorsolaterally from the ventral side of the terminal pharyngeal bulb towards the lateral hypodermis. In wild-type animals, when the canals reach the lateral hypodermis they cross the hypodermal basement membrane and bifurcate, sending processes anteriorly to the head and posteriorly to the tail (Nelson et al., 1983) (Fig. 4A).

By contrast, although the excretory cell body is positioned normally in *unc-53(n166)* animals, both the anterior and posterior canals are severely truncated. In the case of the anterior processes, they terminate close to the excretory cell body, often not extending further than the anterior pharyngeal bulb, while the majority of posterior canals grow out approximately half way, terminating at the level of the vulva (Fig. 4B). These phenotypes were also observed

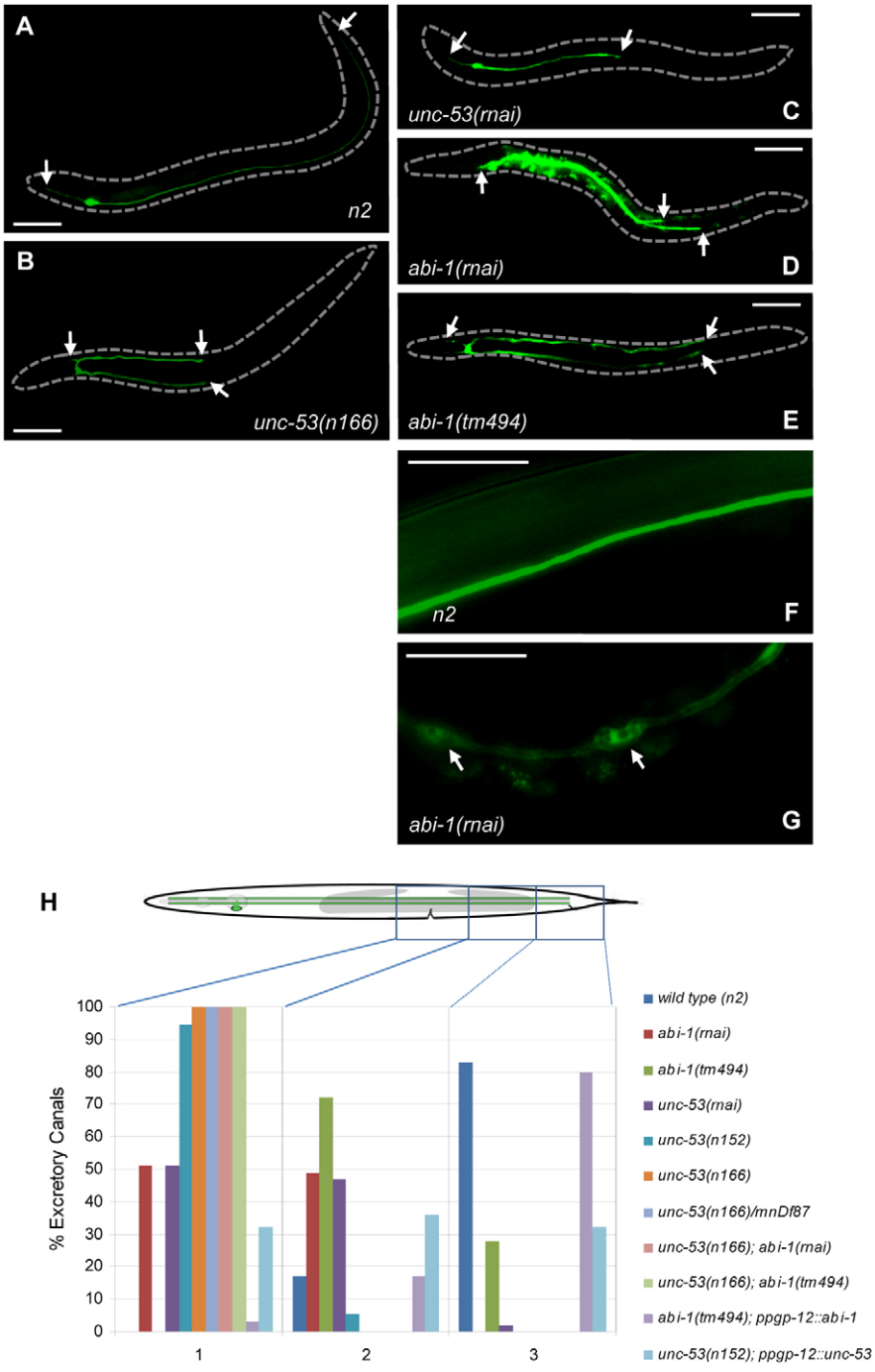

Fig. 4. Excretory canal morphology in wild-type, *unc-53* and *abi-1* animals. (**A-G**) Fluorescence micrographs of hermaphrodites carrying the *ppgp-12::gfp* transgene, allowing for the visualization of the excretory cell body and canals (anterior and posterior termini marked by arrows, A-E). Anterior is to the left and animals are displayed laterally with the exception of B and E, which are shown ventrally. (A) Morphology of the wild-type excretory cell body and processes. The excretory cell body is positioned on the ventral side of the posterior pharyngeal bulb and extends two canals towards the anterior of the animal to the tip of the head and two canals posteriorly to the tail. (B) *unc-53(n166).* (C) *unc-53(rnai).* (D) *abi-1(rnai).* (E) *abi-1(tm494).* (F,G) Lateral view of wild-type excretory canal (F) and *abi-1(rnai)* canal (G), showing numerous small cysts (arrows). (**H**) Quantification of posterior excretory canal outgrowth defects. The outgrowth of the posterior canals was divided into three regions (1-3) between the vulva and the tail as shown. The stop point of canals was determined by fluorescence microscopy for wild type (*n*=72), *abi-1(rnai)* (*n*=141), *abi-1(tm494)* (*n*=116), *unc-53(rnai)* (*n*=87), *unc-53(n152)* (*n*=37), *unc-53(n166)* (*n*=55), *unc-53(n166)/mnDf87* (*n*=107), *unc-53(n166); abi-1(rnai)* (*n*=55), *unc-53(n166); abi-1(tm494)* (*n*=55), *abi-1(tm494); ppgp-12::abi-1* (*n*=51) and *unc-53(n152); ppgp-12::unc-53L* (*n*=28). Scale bars: 100 μm.

by *unc-53(rnai)* and in *unc-53(n152)* mutants (Fig. 4C,H). Notably, defects in the posterior migrations of the excretory canals in *unc-53(n166)* animals were equally as strong as in heterozygous *n166/mnDf87* worms (Fig. 4H), suggesting that *unc-53(n166)*, which removes a coiled-coil domain, an LKK motif and the AAA cassette from all isoforms (Fig. 1B), is a null allele for this phenotype. To determine the role of *abi-1* in excretory cell migration, we examined the length of canals in *abi-1(tm494)* and by RNAi. Animals carrying the *abi-1(tm494)* deletion are superficially wild type, with the exception of a mild uncoordination defect, characterized by an increased frequency of backing. Although the cell body of the excretory cell in *abi-1(tm494)* is positioned normally, examination of the posterior excretory canals of *tm494* revealed a failure of the majority to exit the gonad region (Fig. 4E,H). The position of the excretory cell body was also normal in *abi-1(rnai)* animals, but a range of migration defects were observed, including truncated anterior and posterior excretory canals (Fig. 4C,H), which is reminiscent of *unc-53* loss-of-function alleles, in addition to dorsoventral defects not observed in *unc-53* mutants (data not shown) and excretory cell cysts (Fig. 4G). Notably, excretory canal defects were observed to be no more severe in *unc-53(n166); abi-1(tm494)* double mutants than in *unc-53(n166)* (Fig. 4H). Although the deletion in *abi-1(tm494)* results in a truncated protein, the *abi-1(tm494)* allele behaves as a hypomorph, as *abi-1(rnai)* exacerbates excretory canal defects in an *abi-1(tm494)* background (data not shown). As is the case for the *abi-1(tm494);*

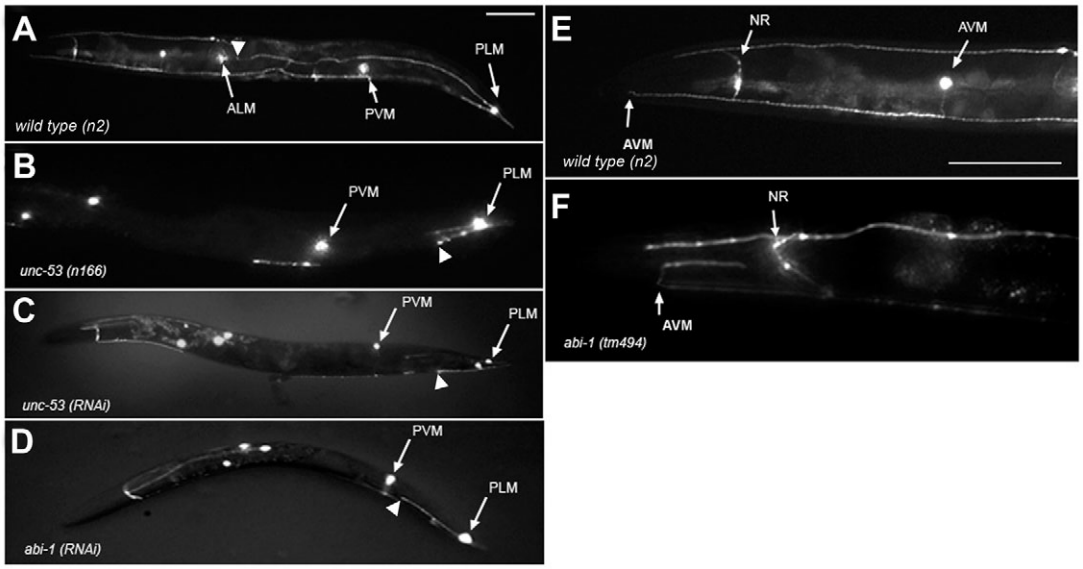

Fig. 5. Mechanosensory neuron phenotype in wild-type, *unc-53* and *abi-1* animals. (**A**) Fluorescence micrograph showing a lateral view of a wild-type hermaphrodite carrying the *pmec-4::gfp* transgene. The PLM, PVM and ALM neuronal cell bodies and axons are shown. The stop point of the PLM axon was scored with respect to the wild-type position near the ALM cell body (arrowheads indicate final position of the PLM axon). (**B**) *unc-53(n166)* animal with truncated PLM and PVM axons. (**C**) *unc-53(rnai)* animal with truncated PLM and PVM axons. (**D**) *abi-1(rnai)* animal showing truncated PLM axon stopping short of the PVM cell body. (**E**) AVM axon in a wild-type animal. AVM axons were considered wild type if they projected anteriorly past the nerve ring (NR) and terminated at the tip of the animal. (**F**) *abi-1(tm494)* animal showing an AVM axon misdirected dorsally (arrow), followed by an abnormal posteriorly directed migration. Scale bars: 100 μm.

unc-53(n166) double mutant, *abi-1(rnai)* in an *unc-53(n166)* background does not reduce the extension of the posterior excretory canals beyond that of *unc-53(n166)* alone (Fig. 4H), suggesting that these genes function within the same pathway to control outgrowth of the posterior excretory canals. Previous work suggests that *unc-53* may function cell autonomously (Stringham et al., 2002), so given the physical interaction observed between UNC-53 and ABI-1, we hypothesized that ABI-1 and UNC-53 may both function within the excretory canals. Consistent with this prediction, full-length *abi-1* and *unc-53* cDNA driven by the *ppgp-12* excretory cell-specific promoter was sufficient to rescue the canal outgrowth defects of *abi-1(tm494)* and *unc-53(n152)* mutants, respectively (Fig. 4H).

To determine whether ABI-1 functions in the migration of axons, we examined the outgrowth of the mechanosensory neurons that control the touch response. The cell bodies and axons of the mechanosensory neurons are reproducibly positioned in wild-type animals, and can be visualized using the cell-specific *pmec-4::gfp* reporter. In wild-type animals, PLML/R cell bodies are positioned within the lumbar ganglia of the tail, where they extend a short posteriorly directed process and a long anteriorly directed axon that grows out along the lateral commissure and terminates near the cell bodies of the ALM neurons (Fig. 5A). By contrast, in *unc-53(n166)* animals, both the anterior and posterior processes are shorter than in wild type. The anterior axons of the PLML/R were prematurely truncated and terminate shortly after beginning their trajectory (Fig. 5B). Similar phenotypes were observed in *unc-53(rnai)* (Fig. 5C). Although no posterior defects were observed in *abi-1(rnai)* animals, a significant number of anteriorly directed PLM axons terminated prematurely at positions posterior to the ALML/R cell bodies (Fig. 5D). None of the PLM axons was shorter in *abi-1(rnai)* animals than in *unc-53(n166)*. In the weak *abi-1(tm494)* allele, outgrowth of PLM was normal but misdirection of the AVM axonal projection was observed (Fig. 5E,F). During wild-type development, the AVM axon undergoes a short ventral migration followed by a turn and migration anteriorly along the ventral cord, where it extends past the nerve ring into the tip of the head (Fig. 5E). In *abi-1(tm494)* animals, the initial ventral and longitudinal anterior migrations of the AVM axons were wild type but, instead of terminating along their anterior trajectory, the AVM would occasionally reroute, turning dorsally away from the ventral cord and then posteriorly back towards the nerve ring (Fig. 5F).

ABI-1 and UNC-53 have overlapping expression patterns

Given the physical interaction between UNC-53 and ABI-1, the shared phenotypes, and because UNC-53 has been shown to function cell autonomously (Stringham et al., 2002), we expected that ABI-1 would be found in the same cells as UNC-53. To determine the expression pattern of ABI-1, we generated transcriptional and translational GFP-reporter fusions of *abi-1* and raised a polyclonal antibody towards a peptide corresponding to amino acids 256 to 274 of ABI-1. Collectively, these approaches revealed that ABI-1 is expressed in a number of neurons within the nerve ring and head, including the amphid interneurons AIYL/R (Fig. 6A), the RMEL/R motoneurons (Fig. 6B), coelomocytes (Fig. 6D), and several classes of ventral cord motoneuron, where it is localized throughout the cell bodies, dendrites and commissural axons extending to the dorsal cord (Fig. 6C), similar to the pattern of expression observed for UNC-53L transcripts (Fig. 1C).

ABI-1 and UNC-53 control dorsoventral migrations of the motoneurons

The expression of both UNC-53 and ABI-1 in motoneurons suggests that both genes may have a role in the guidance and outgrowth of these cells. Consistent with this, RNAi of *abi-1* revealed multiple

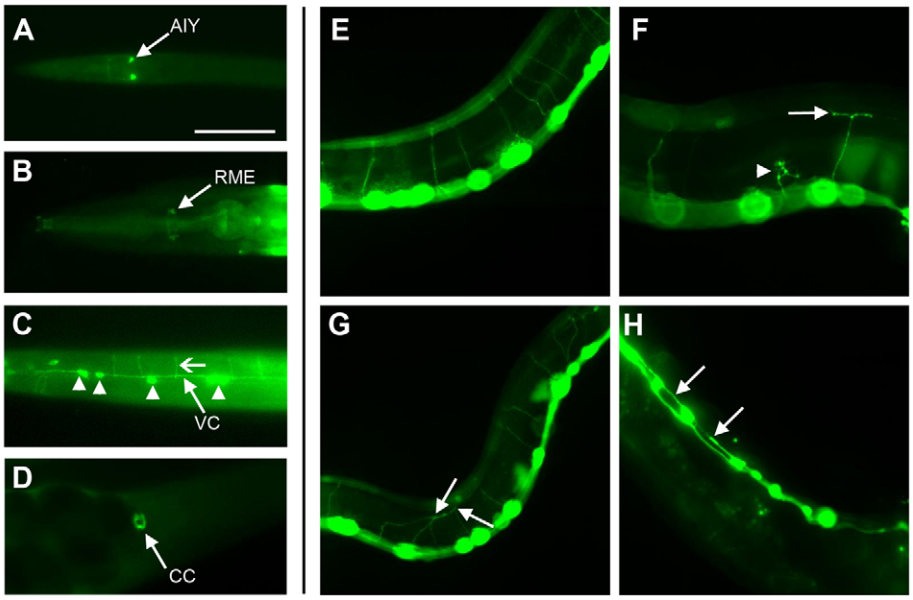

Fig. 6. ABI-1 expression and motoneuron migration defects. (**A-D**) Expression pattern of ABI-1. (A) Head of a larva expressing *pabi-1::gfp* in the AIYL/R neurons. (B,C) Expression of ABI-1 detected by immunostaining with *PAb-ABI-1*. (B) Head of a wild-type animal showing ABI-1 expression in the nerve ring and in the cell bodies of the RMEL/R neurons (arrow). (C) Ventral surface of the midbody of an adult worm showing ABI-1 in the cell bodies of motoneurons (arrowheads), in addition to the longitudinal tracts of the ventral cord (VC) and the dorsal commissures (arrow). (D) Expression of ABI-1 in coelomocyte (CC). (**E-H**) Fluorescence micrographs showing wild-type (E) and *abi-1(rnai)* (F-H) animals. Ventral is down in all cases except H. (E) Wild-type animal with motoneuron cell bodies located ventrally and dorsal commissures extending to the dorsal cord. (F) *abi-1(rnai)* animal showing a truncated and misguided dorsal commissure (arrowhead), and a truncated dorsal commissure with anterior and posterior ectopic lateral branches (arrow). (G) Misrouting and branching of dorsal commissures (arrows). (H) Ventral view of the ventral cord of an *abi-1(rnai)* animal showing marked defasciculation (arrows). Scale bars: 50 μm.

defects in motoneurons, including the presence of ectopic branches in commissures, giving rise to disorganized neural networks (Fig. 6F,G). Frequently, dorsally directed axons were unable to complete their migration to the dorsal cord (32%, *n*=90) and either bifurcated prematurely, extending lateral processes anteriorly and posteriorly, or produced several knob-like structures in disoriented processes, which was suggestive of growth cone stalling (Fig. 6F). Defasciculation of the ventral cord was also frequently observed (13%, *n*=90; Fig. 6H). Similar phenotypes have been reported in *unc-53*, where approximately 13% of motoneuron commissures are abnormal and fail to reach the dorsal cord (Stringham et al., 2002).

Disruption of UNC-53L causes defects in cell outgrowth

Although the N terminus of UNC-53 inclusive of a CH domain is sufficient to bind ABI-1 in vitro, this region is absent in short UNC-53 isoforms (Stringham et al., 2002). To determine whether the long-isoform of UNC-53 is required for posterior EC migration, we directed RNAi toward exons 1-4 of UNC-53 and found that knockdown of UNC-53L is sufficient to impair longitudinal guidance even with the short isoforms present (Fig. 7A), a finding that is consistent with UNC-53L function and expression in the EC. To test further whether the interaction between UNC-53 and ABI-1 is functionally important, we overexpressed the CH domain of UNC-53L in the excretory cell. At a low frequency, various canal defects were observed, including ectopic outgrowths, cysts and the truncation of posterior canals (Fig. 7B-D), phenotypes that are reminiscent of *abi-1* knockdown. This suggests that expression of the CH domain alone may act in a dominant-negative fashion to sequester endogenous ABI-1 and prevent functional interaction with wild-type UNC-53 in vivo.

Mutations in actin-polymerization proteins disrupt longitudinal migration

The extension of cellular processes is mediated primarily through the extension of growth cones, highly motile ends at cell tips that are undergoing constant cytoskeletal reorganization. ABI-1 functions in cytoskeletal organization through its ability to regulate the ARP2/3 complex to induce actin polymerization. Evidence suggests that ABI-1 may regulate ARP2/3 through a complex with WAVE in response to RAC (Bompard and Caron, 2004; Stradal et al., 2004) or by binding WASP (Innocenti et al., 2002). To test whether these and other proteins known to function with ABI-1 are involved in longitudinal migration in *C. elegans*, we analyzed the excretory canal phenotypes of mutant and RNAi-treated animals. Of the genes tested, *wve-1(rnai)*, *nck-1(ok694)* and *arx-2(rnai)* produced excretory canal migration phenotypes reminiscent of *unc-53* and *abi-1* mutants (Fig. 8), while *wsp-1* and *abl-1* did not. Notably, none of the genes tested had more severe phenotypes either alone or in the background of the null *unc-53* allele *(n166)*, suggesting that the initial trajectory of the posterior excretory canals to the anterior gonad arm is unaffected by loss of *unc-53*, *abi-1* or known *abi-1* interactors. Interestingly, *nck-1* is expressed in the excretory cell and ventral cord motoneurons (Fig. 9), two cell types affected in *unc-53* and *abi-1* mutant backgrounds. We also examined the potential role of these proteins in the migration of PLM axons and found that RNAi had modest effects (Table 1).

DISCUSSION

A role for ABI-1 in cell migration and growth cone extension

In this study, ABI-1 was localized to the cytoplasm of ventral cord motoneurons, as well as to commissures that span the dorsoventral axis and innervate the dorsal cord. The expression pattern is

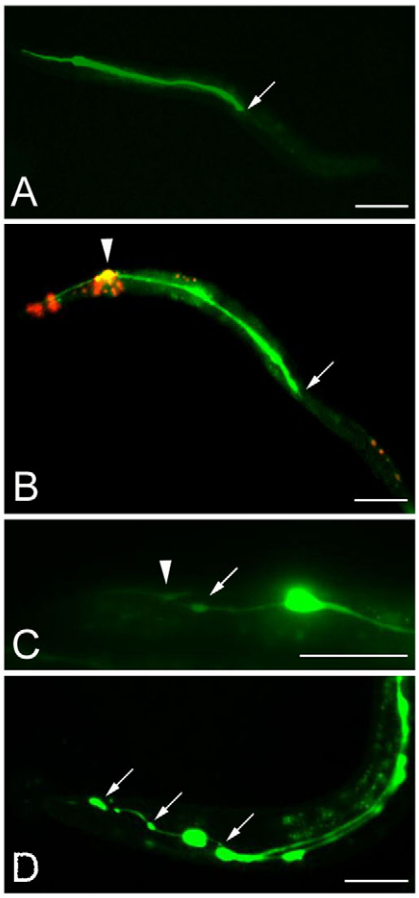

Fig. 7. RNAi of the long isoform of UNC-53 and overexpression of the UNC-53 CH domain generates excretory cell defects. (**A**) RNAi directed toward the long isoform of *unc-53* results in posterior canal migration, with posterior excretory canals terminating at the vulva (arrow). Three percent of animals had canals terminating at the vulva and 24% failed to exit past the posterior gonad arm (n=92). (**B**) Adult animal expressing *ppgp12::unc-53CH::gfp* in the excretory cell body, as indicated by merge (yellow, arrowhead) with dsRED co-injection marker *pDPY-30::NLS::DSRED2*, displays a posterior excretory canal truncated at the midbody position near the vulva (arrow). Seven percent of canals terminate near the vulva and 22% failed to exit the posterior gonad arm (n=116). (**C**,**D**) Defects of the excretory canals in adult animals expressing *ppgp-12::unc-53CH::gfp* in the excretory canal. (C) Head of an adult animal showing cysts (arrow) and ectopic anterior branches (arrowhead). (D) Adult animal showing various excretory canal cysts (arrows). Scale bars: 100 μm.

consistent with a role for ABI-1 in nervous system development, and is confirmed by the guidance defects observed in the motoneurons of *abi-1* animals. In mammals, ABI proteins are highly expressed in the developing brain, where they guide nerve cell placement and axon outgrowth (Courtney et al., 2000; Grove et al., 2004). ABI-1 localizes to the motile tips of lamellipodia and filopodia, which is consistent with a role for ABI-1 in actin-polymerization events (Echarri et al., 2004; Stradal et al., 2001). Surprisingly, ABI-1 expression was not seen in the excretory cell as had been expected given the physical interaction between UNC-53 and ABI-1, and because UNC-53 is expressed in the EC (Stringham et al., 2002). It is possible that endogenous levels of ABI-1 are very low and/or that sequences required for expression in these cells were absent in the reporter fusions. Nonetheless, the ability of both ABI-1 and UNC-53 to rescue outgrowth when expressed specifically in the excretory cell, coupled with the finding that disruption of the UNC-53–ABI-1 interaction interfered with canal outgrowth, strongly suggest that ABI-1 and UNC-53 function together in the excretory cell.

The expression of both ABI-1 and UNC-53 in motoneurons, and the observation that loss of *abi-1* and *unc-53* function disrupts the dorsal outgrowth of motoneuron commissures suggests that these genes may participate together in dorsoventral guidance decisions. A role for the navigators, vertebrate homologs of UNC-53, in dorsal ventral guidance is also apparent. Mouse NAV1 is expressed in neurons that migrate along both the longitudinal and dorsoventral axes during development, and rat pontine neuronal explants are unable to respond to the netrin 1 guidance cue when mouse NAV1 is knocked down by RNAi (Martinez-Lopez et al., 2005). Circumferential guidance of growth cones in *C. elegans* is controlled by multiple guidance cues, including UNC-6/netrin, which is expressed ventrally, where it attracts UNC-40/DCC-expressing growth cones and repels those expressing both UNC-40 and UNC-5 (Wadsworth, 2002). Interestingly, UNC-34/Ena, which controls multiple aspects of cell migration and guidance (Gitai et al., 2003; Shakir et al., 2006; Withee et al., 2004; Yu et al., 2002), can suppress ectopic UNC-5 expression, placing UNC-34 downstream of UNC-5 in circumferential guidance (Colavita and Culotti, 1998). Mammalian Ena function is partially dependent on ABI proteins, and could suggest a role for ABI-1 in circumferential guidance in worms. (Comer et al., 1998; Juang and Hoffmann, 1999; Tani et al., 2003).

ABI-1 interactors and ARP2/3 control longitudinal migration

The migration defects observed in both *abi-1* and *unc-53* mutants is consistent with the biochemical interaction observed between them. Moreover, the phenotype of the ABI-1 interactor *nck-1* in the excretory cell suggests a similar role for *nck-1*. The adaptor NCK-1 exerts its influence in part through the modulation of WVE-1, as NCK-1 and/or RAC activation is able to release SCAR-1 from an inhibitory complex containing ABI-2 to activate the ARP2/3 complex (Eden et al., 2002). Therefore, it was not surprising that similar longitudinal guidance phenotypes were also observed in *wve-1* and *arx-2*, suggesting that the primary mode of *unc-53* action in these migrations is mediated through conserved interactions. Consistent with this view, both UNC-53 and the RAC activator UNC-73/TRIO have been implicated in an EGL-17/FGF-independent signaling mechanism controlling sex myoblast migration (Chen et al., 1997), suggesting that modulation of the ARP2/3 complex may be the crucial determinant of actin filament assembly in this migration as well. Interestingly, the first part of the posteriorly directed migration of the excretory canals to the anterior gonad arm was intact for all genes tested, suggesting that another mechanism independent of *unc-53*, *abi-1* and the ARP2/3 complex might be driving the initial posterior outgrowth of the canals.

Experiments in both cell culture and model systems reveal that cell shape changes, and the extension of cellular processes are mediated through GTPases of the RHO family, including CDC42 and RAC, which induce the formation of lamellipodia and filopodia by interacting directly or indirectly with the WASP family of proteins, resulting in the activation of the ARP2/3 complex and directed actin nucleation (Bompard and Caron, 2004; Stradal et al., 2004; Takenawa and Suetsugu, 2007). For example, in *C. elegans*, loss of WSP-1 or WVE-1 disrupts hypodermal cell migration and ventral enclosure during embryogenesis, phenotypes that are also characteristic of CED-10/RAC-1 mutants (Lundquist et al., 2001) and ARP2/3-complex knockdown (Sawa et al., 2003). Moreover, the motoneuron guidance

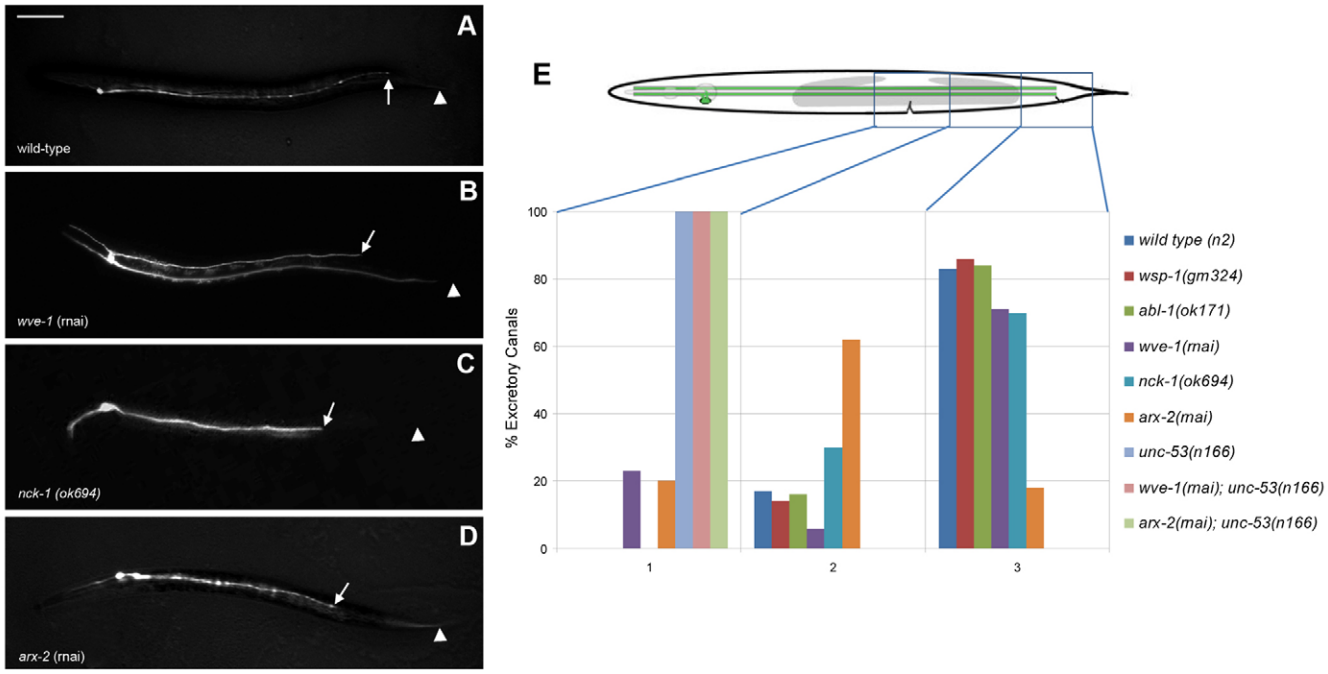

Fig. 8. Excretory cell morphology in wild type, *wve-1(rnai), nck-1(ok694) and arx-2(rnai)* animals. (**A-D**) Fluorescence micrographs of hermaphrodites carrying the *ppgp-12::gfp* transgene. The final positions of the posterior excretory canals are marked by arrows and the anus is marked by arrowheads. Lateral views are shown in all cases except for B, which is a ventral view. Anterior is to the left. Scale bars: 100 μm. (A) Wild-type animal with posterior canals terminating near the anus. (B-D) RNAi-treated and mutant animals, as indicated have posterior excretory canals that stop anterior to their wild-type positions (arrows). (**E**) Quantification of posterior longitudinal migration defects. Wild type (*n*=72), *wsp-1(gm324)* (*n*=69), *abl-1(ok171)* (*n*=77), *wve-1(rnai)* (*n*=173), *nck-1(ok694)* (*n*=50), *arx-2(rnai)* (*n*=137), *unc-53(n166)* (*n*=55), *wve-1(rnai); unc-53(n166)* (*n*=90), *arx-2(rnai); unc-53(n166)* (*n*=91).

defects observed in *unc-53* and *abi-1* animals are similar to those observed in *ced-10* and *wve-1* (Lundquist et al., 2001; Lundquist, 2003; Withee et al., 2004), consistent with a model in which these proteins operate together in cytoskeletal remodelling. ABI-1 is a member of a complex consisting of WAVE-1 (WVE-1), GEX-2, GEX-3 and HSPC300 that promotes actin nucleation (Innocenti et al., 2004; Stroschein-Stevenson et al., 2006). The defects in cell movements during morphogenesis reported for *gex-2* and *gex-3* (Soto et al., 2002), and the similarities in the phenotypes of *abi-1* and *wve-1* reported here are consistent with a model in which these proteins form a similar complex in *C. elegans*.

Two models of ARP2/3 complex activation have been proposed; one that relies on WAVE and another that relies on WASP (Bompard and Caron, 2004; Stradal et al., 2004). ABI-1 seems to participate in both, binding through its N terminus to WAVE to regulate membrane protrusion and macropinocytosis, and through its SH3 domain to N-WASP to stimulate actin-dependent vesicular transport and endocytosis (Innocenti et al., 2005). Thus ABI-1 may be a central figure that regulates the proportion of actin filament nucleation designated for particular processes by partitioning WASP versus WAVE activation (Innocenti et al., 2005). Our results indicate an essential role for WAVE as opposed to WASP in longitudinal outgrowth in *C. elegans*.

A model for UNC-53–ABI-1 action

Previously, it was shown that UNC-53 interacts physically with SEM-5/GRB2 (Stringham et al., 2002), a SH2-SH3 adapter involved in multiple RTK pathways, including FGFR (Dixon et al., 2006), EGFR (Moghal and Sternberg, 2003), and IR (Hopper, 2006) signaling. At present, it is unclear whether UNC-53 is a participant in one or several signaling cascades. For example, whereas both *unc-53* and *egl-15/FGFR* are expressed in the migrating sex myoblasts (Goodman et al., 2003), *egl-15* is not expressed in axons (where it regulates outgrowth) but instead exerts its effect through the underlying hypodermis on which they migrate (Bulow et al., 2004). As UNC-53 is a cytoplasmic protein that functions cell autonomously, this suggests that it does not act directly downstream of EGL-15/FGFR signaling in neuronal cell migrations, but that it might be recruited by a different receptor upstream of SEM-5/GRB2. Moreover, UNC-53, the cell-adhesion molecule UNC-71/ADAM and UNC-73/TRIO, have all

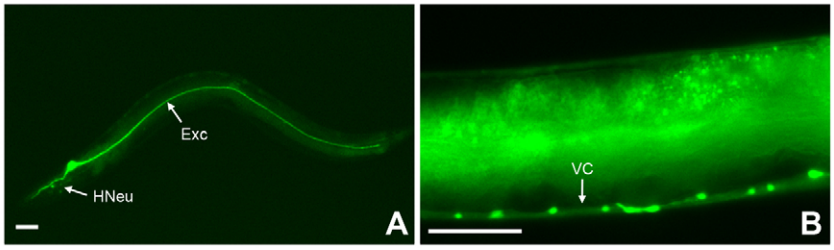

Fig. 9. Expression pattern of *nck-1* using *pnck-1::gfp*. (**A**) Adult hemaphrodite showing expression in the excretory cell (Exc) and head neurons (HNeu). (**B**) View of the midbody of adult hemaphrodite showing expression in several motoneurons of the ventral cord (VC). Scale bars: 50 μm.

Table 1. Percentage of anteriorly directed PLM axons truncated in *eri-1(mg366); pmec-4::gfp*

Genotype	Percentage of truncated PLM axons	*n*
wild type *(n2)*	0.8	114
unc-53(n166)	100	114
unc-53(rnai)	15	130
abi-1(rnai)	9.6	137
nck-1(rnai)	4	102
arx-2(rnai)	11	104

been implicated in a EGL-17/FGF-independent signaling mechanism controlling sex myoblast migrations (Chen et al., 1997), suggesting non-FGFR signaling is involved in this pathway as well. Therefore the identity of ligands and receptors upstream of the SEM-5/UNC-53 interaction in cell migration remain elusive.

In this study, we found that a restricted region of the N terminus of UNC-53 containing a CH domain was sufficient to bind ABI-1 in vitro, and that the UNC-53–ABI-1 interaction mediated by this domain is required for longitudinal cell outgrowth in vivo. CH domains are commonly found in proteins involved in signal transduction and actin binding, and are classified by the number and position of CH domains they contain (Korenbaum and Rivero, 2002). Type 1/2 CH domain proteins, such as α-actinin, β-spectrin and dystrophin, which function in actin bundling and membrane anchoring (Broderick and Winder, 2005), possess two N-terminal CH domains in tandem. The first Type 1 CH domain mediates actin binding, whereas the second Type 2 CH domain may (1) stabilize the actin interaction of the Type I domain, (2) localize the actin-binding protein to the cytoskeleton, or (3) act as a scaffold for signal transduction (Gimona et al., 2002). By contrast, UNC-53 possesses a single N-terminal CH domain, and in this respect is more closely related to Type 3 CH domain-containing proteins, such as VAV, IQGAP, αPIX and SM22 (Gimona et al., 2002; Stradal et al., 1998). Type 3 CH domains function like Type 2 CH domains in that they act as scaffolds that bind proteins involved in the control of cytoskeletal change and signal transduction (Galkin et al., 2006; Gimona and Mital, 1998; Korenbaum and Rivero, 2002; Leinweber et al., 1999). In such a model, UNC-53 may be a scaffold that coordinates upstream signals transduced through SEM-5/GRB2 to ABI-1 and the actin cytoskeleton.

The complexity of the *unc-53* locus gives rise to several protein isoforms that are regulated by different promoters and that display non-overlapping tissue-specific expression patterns (Choi and Newman, 2006; Stringham et al., 2002). The smaller isoforms are under the control of intronic promoters, producing polypeptides that lack CH domains, which might limit their ability to interact with ABI-1 and significantly alter their function. Interestingly, both murine and human NAV1 also lack CH domains (unlike mouse and human NAV2 and NAV3), and are the only NAV genes downregulated in brain following development (Maes et al., 2002; Peeters et al., 2004), suggesting a possible post-developmental role for the NAVs possessing CH domains. Understanding the relationship between the tissue specificity and the domain organization of the various isoforms of UNC-53 and the vertebrate NAVs should shed light on the importance of the CH domains in these proteins and how they operate.

We thank Laura Ramsay, Erin Kreiter, Will Bronec, Tanya Martens and Samantha Grainger for technical assistance; the *Caenorhabitis* Genetics Centre, Monica Driscoll, Shohei Mitani and Harald Hutter for nematode strains; and Bob Barstead for the *C. elegans* yeast two-hybrid library. We are grateful to Nancy Hawkins, Christopher Beh, and members of the Stringham and Baillie labs for helpful discussions. J.W. was the recipient of an NSERC USRA. This work was supported by NSERC Discovery Grants to E.G.S. and to D.B., and by the Canada Research Chairs to E.G.S. and D.B.

References

Aspenstrom, P. and Olson, M. F. (1995). Yeast two-hybrid system to detect protein-protein interactions with Rho GTPases. *Methods Enzymol.* **256**, 228-241.
Bettinger, J. C., Lee, K. and Rougvie, A. E. (1996). Stage-specific accumulation of the terminal differentiation factor LIN-29 during *Caenorhabditis elegans* development. *Development* **122**, 2517-2527.
Birnbaum, D., Popovici, C. and Roubin, R. (2005). A pair as a minimum: the two fibroblast growth factors of the nematode *Caenorhabditis elegans*. *Dev. Dyn.* **232**, 247-255.
Bompard, G. and Caron, E. (2004). Regulation of WASP/WAVE proteins: making a long story short. *J. Cell Biol.* **166**, 957-962.
Brenner, S. (1974). The genetics of *Caenorhabditis elegans*. *Genetics* **77**, 71-94.
Broderick, M. J. and Winder, S. J. (2005). Spectrin, alpha-actinin, and dystrophin. *Adv. Protein Chem.* **70**, 203-246.
Bulow, H. E., Boulin, T. and Hobert, O. (2004). Differential functions of the *C. elegans* FGF receptor in axon outgrowth and maintenance of axon position. *Neuron* **42**, 367-374.
Burdine, R. D., Chen, E. B., Kwok, S. F. and Stern, M. J. (1997). *egl-17* encodes an invertebrate fibroblast growth factor family member required specifically for sex myoblast migration in *Caenorhabditis elegans*. *Proc. Natl. Acad. Sci. USA* **94**, 2433-2437.
Chen, E. B., Branda, C. S. and Stern, M. J. (1997). Genetic enhancers of *sem-5* define components of the gonad-independent guidance mechanism controlling sex myoblast migration in *Caenorhabditis elegans* hermaphrodites. *Dev. Biol.* **182**, 88-100.
Choi, J. and Newman, A. P. (2006). A two-promoter system of gene expression in *C. elegans*. *Dev. Biol.* **296**, 537-544.
Colavita, A. and Culotti, J. G. (1998). Suppressors of ectopic UNC-5 growth cone steering identify eight genes involved in axon guidance in *Caenorhabditis elegans*. *Dev. Biol.* **194**, 72-85.
Comer, A. R., Ahern-Djamali, S. M., Juang, J. L., Jackson, P. D. and Hoffmann, F. M. (1998). Phosphorylation of Enabled by the *Drosophila* Abelson tyrosine kinase regulates the *in vivo* function and protein-protein interactions of Enabled. *Mol. Cell. Biol.* **18**, 152-160.
Cordes, S., Frank, C. A. and Garriga, G. (2006). The *C. elegans* MELK ortholog PIG-1 regulates cell size asymmetry and daughter cell fate in asymmetric neuroblast divisions. *Development* **133**, 2747-2756.
Courtney, K. D., Grove, M., Vandongen, H., Vandongen, A., LaMantia, A. S. and Pendergast, A. M. (2000). Localization and phosphorylation of Abl-interactor proteins, *abi-1* and *abi-2*, in the developing nervous system. *Mol. Cell. Neurosci.* **16**, 244-257.
Dai, Z. and Pendergast, A. M. (1995). Abi-2, a novel SH3-containing protein interacts with the c-Abl tyrosine kinase and modulates c-Abl transforming activity. *Genes Dev.* **9**, 2569-2582.
DeVore, D. L., Horvitz, H. R. and Stern, M. J. (1995). An FGF receptor signaling pathway is required for the normal cell migrations of the sex myoblasts in *C. elegans* hermaphrodites. *Cell* **83**, 611-620.
Dixon, S. J., Alexander, M., Fernandes, R., Ricker, N. and Roy, P. J. (2006). FGF negatively regulates muscle membrane extension in *Caenorhabditis elegans*. *Development* **133**, 1263-1275.
Echarri, A., Lai, M. J., Robinson, M. R. and Pendergast, A. M. (2004). Abl interactor 1 (*abi-1*) Wave-binding and SNARE domains regulate its nucleocytoplasmic shuttling, lamellipodium localization, and Wave-1 levels. *Mol. Cell. Biol.* **24**, 4979-4993.
Eden, S., Rohatgi, R., Podtelejnikov, A. V., Mann, M. and Kirschner, M. W. (2002). Mechanism of regulation of WAVE1-induced actin nucleation by Rac1 and Nck. *Nature* **418**, 790-793.
Frangioni, J. V. and Neel, B. G. (1993). Solubilization and purification of enzymatically active glutathione S-transferase (pGEX) fusion proteins. *Anal. Biochem.* **210**, 179-187.
Funato, Y., Terabayashi, T., Suenaga, N., Seiki, M., Takenawa, T. and Miki, H. (2004). IRSp53/Eps8 complex is important for positive regulation of Rac and cancer cell motility/invasiveness. *Cancer Res.* **64**, 5237-5244.
Galkin, V. E., Orlova, A., Fattoum, A., Walsh, M. P. and Egelman, E. H. (2006). The CH-domain of calponin does not determine the modes of calponin binding to F-actin. *J. Mol. Biol.* **359**, 478-485.
Ghenea, S., Boudreau, J. R., Lague, N. P. and Chin-Sang, I. D. (2005). The VAB-1 Eph receptor tyrosine kinase and SAX-3/Robo neuronal receptors function together during *C. elegans* embryonic morphogenesis. *Development* **132**, 3679-3690.
Gimona, M. and Mital, R. (1998). The single CH domain of calponin is neither sufficient nor necessary for F-actin binding. *J. Cell. Sci.* **111**, 1813-1821.
Gimona, M., Djinovic-Carugo, K., Kranewitter, W. J. and Winder, S. J. (2002). Functional plasticity of CH domains. *FEBS Lett.* **513**, 98-106.
Gitai, Z., Yu, T. W., Lundquist, E. A., Tessier-Lavigne, M. and Bargmann, C. I. (2003). The Netrin receptor UNC-40/DCC stimulates axon attraction and outgrowth through Enabled and, in parallel, Rac and UNC-115/AbLIM. *Neuron* **37**, 53-65.

Goodman, S. J., Branda, C. S., Robinson, M. K., Burdine, R. D. and Stern, M. J. (2003). Alternative splicing affecting a novel domain in the *C. elegans* EGL-15 FGF receptor confers functional specificity. *Development* **130**, 3757-3766.
Grove, M., Demyanenko, G., Echarri, A., Zipfel, P. A., Quiroz, M. E., Rodriguiz, R. M., Playford, M., Martensen, S. A., Robinson, M. R., Wetsel, W. C. et al. (2004). ABI2-deficient mice exhibit defective cell migration, aberrant dendritic spine morphogenesis, and deficits in learning and memory. *Mol. Cell. Biol.* **24**, 10905-10922.
Hao, J. C., Yu, T. W., Fujisawa, K., Culotti, J. G., Gengyo-Ando, K., Mitani, S., Moulder, G., Barstead, R., Tessier-Lavigne, M. and Bargmann, C. I. (2001). *C. elegans* Slit acts in midline, dorsal-ventral, and anterior-posterior guidance via the SAX-3/Robo receptor. *Neuron* **32**, 25-38.
Hedgecock, E. M., Culotti, J. G. and Hall, D. H. (1990). The *unc-5, unc-6*, and *unc-40* genes guide circumferential migrations of pioneer axons and mesodermal cells on the epidermis in *C. elegans*. *Neuron* **4**, 61-85.
Hekimi, S. and Kershaw, D. (1993). Axonal guidance defects in a *Caenorhabditis elegans* mutant reveal cell-extrinsic determinants of neuronal morphology. *J. Neurosci.* **13**, 4254-4271.
Higgs, H. N. and Pollard, T. D. (2000). Activation by Cdc42 and PIP(2) of Wiskott-Aldrich syndrome protein (WASp) stimulates actin nucleation by Arp2/3 complex. *J. Cell Biol.* **150**, 1311-1320.
Hopper, N. A. (2006). The adaptor protein Soc-1/Gab1 modifies growth factor receptor output in *Caenorhabditis elegans*. *Genetics* **173**, 163-175.
Ibarra, N., Pollitt, A. and Insall, R. H. (2005). Regulation of actin assembly by SCAR/WAVE proteins. *Biochem. Soc. Trans.* **33**, 1243-1246.
Innocenti, M., Tenca, P., Frittoli, E., Faretta, M., Tocchetti, A., Di Fiore, P. P. and Scita, G. (2002). Mechanisms through which Sos-1 coordinates the activation of Ras and Rac. *J. Cell Biol.* **156**, 125-136.
Innocenti, M., Zucconi, A., Disanza, A., Frittoli, E., Areces, L. B., Steffen, A., Stradal, T. E., Di Fiore, P. P., Carlier, M. F. and Scita, G. (2004). Abi-1 is essential for the formation and activation of a WAVE2 signaling complex. *Nat. Cell Biol.* **6**, 319-327.
Innocenti, M., Gerboth, S., Rottner, K., Lai, F. P., Hertzog, M., Stradal, T. E., Frittoli, E., Didry, D., Polo, S., Disanza, A. et al. (2005). Abi-1 regulates the activity of N-WASP and WAVE in distinct actin-based processes. *Nat. Cell Biol.* **7**, 969-976.
Ishii, N., Wadsworth, W. G., Stern, B. D., Culotti, J. G. and Hedgecock, E. M. (1992). UNC-6, a laminin-related protein, guides cell and pioneer axon migrations in *C. elegans*. *Neuron* **9**, 873-881.
Jenei, V., Andersson, T., Jakus, J. and Dib, K. (2005). E3B1, a human homologue of the mouse gene product *abi-1*, sensitizes activation of Rap1 in response to epidermal growth factor. *Exp. Cell Res.* **310**, 463-473.
Juang, J. L. and Hoffmann, F. M. (1999). *Drosophila* Abelson interacting protein (dAbi) is a positive regulator of Abelson tyrosine kinase activity. *Oncogene* **18**, 5138-5147.
Kamath, R. S., Martinez-Campos, M., Zipperlen, P., Fraser, A. G. and Ahringer, J. (2001). Effectiveness of specific RNA-mediated interference through ingested double-stranded RNA in *Caenorhabditis elegans*. *Genome Biol.* **2**, RESEARCH0002.
Kennedy, S., Wang, D. and Ruvkun, G. (2004). A conserved siRNA-degrading RNase negatively regulates RNA interference in *C. elegans*. *Nature* **427**, 645-649.
Kishi, M., Kummer, T. T., Eglen, S. J. and Sanes, J. R. (2005). LL5beta: a regulator of postsynaptic differentiation identified in a screen for synaptically enriched transcripts at the neuromuscular junction. *J. Cell Biol.* **169**, 355-366.
Korenbaum, E. and Rivero, F. (2002). Calponin homology domains at a glance. *J. Cell. Sci.* **115**, 3543-3545.
Leinweber, B. D., Leavis, P. C., Grabarek, Z., Wang, C. L. and Morgan, K. G. (1999). Extracellular regulated kinase (ERK) interaction with actin and the calponin homology (CH) domain of actin-binding proteins. *Biochem. J.* **344**, 117-123.
Levy-Strumpf, N. and Culotti, J. G. (2007). VAB-8, UNC-73 and MIG-2 regulate axon polarity and cell migration functions of UNC-40 in *C. elegans*. *Nat. Neurosci.* **10**, 161-168.
Lundquist, E. A. (2003). Rac proteins and the control of axon development. *Curr. Opin. Neurobiol.* **13**, 384-390.
Lundquist, E. A., Reddien, P. W., Hartwieg, E., Horvitz, H. R. and Bargmann, C. I. (2001). Three *C. elegans* Rac proteins and several alternative Rac regulators control axon guidance, cell migration and apoptotic cell phagocytosis. *Development* **128**, 4475-4488.
Maes, T., Barcelo, A. and Buesa, C. (2002). Neuron navigator: a human gene family with homology to *unc-53*, a cell guidance gene from *Caenorhabditis elegans*. *Genomics* **80**, 21-30.
Martinez-Lopez, M. J., Alcantara, S., Mascaro, C., Perez-Branguli, F., Ruiz-Lozano, P., Maes, T., Soriano, E. and Buesa, C. (2005). Mouse Neuron Navigator 1, a novel microtubule-associated protein involved in neuronal migration. *Mol. Cell. Neurosci.* **28**, 599-612.
McKay, S. J., Johnsen, R., Khattra, J., Asano, J., Baillie, D. L., Chan, S., Dube, N., Fang, L., Goszczynski, B., Ha, E. et al. (2003). Gene expression profiling of cells, tissues, and developmental stages of the nematode *C. elegans*. *Cold Spring Harb. Symp. Quant. Biol.* **68**, 159-169.
Merrill, R. A., Plum, L. A., Kaiser, M. E. and Clagett-Dame, M. (2002). A mammalian homolog of *unc-53* is regulated by all-trans retinoic acid in neuroblastoma cells and embryos. *Proc. Natl. Acad. Sci. USA* **99**, 3422-3427.
Moghal, N. and Sternberg, P. W. (2003). The epidermal growth factor system in *Caenorhabditis elegans*. *Exp. Cell Res.* **284**, 150-159.
Nelson, F. K., Albert, P. S. and Riddle, D. L. (1983). Fine structure of the *Caenorhabditis elegans* secretory-excretory system. *J. Ultrastruct. Res.* **82**, 156-171.
Pan, C. L., Howell, J. E., Clark, S. G., Hilliard, M., Cordes, S., Bargmann, C. I. and Garriga, G. (2006). Multiple Wnts and Frizzled receptors regulate anteriorly directed cell and growth cone migrations in *Caenorhabditis elegans*. *Dev. Cell.* **10**, 367-377.
Peeters, P. J., Baker, A., Goris, I., Daneels, G., Verhasselt, P., Luyten, W. H., Geysen, J. J., Kass, S. U. and Moechars, D. W. (2004). Sensory deficits in mice hypomorphic for a mammalian homologue of *unc-53*. *Brain Res. Dev. Brain Res.* **150**, 89-101.
Sawa, M. and Takenawa, T. (2006). *Caenorhabditis elegans* WASP-interacting protein homologue WIP-1 is involved in morphogenesis through maintenance of WSP-1 protein levels. *Biochem. Biophys. Res. Commun.* **340**, 709-717.
Sawa, M., Suetsugu, S., Sugimoto, A., Miki, H., Yamamoto, M. and Takenawa, T. (2003). Essential role of the *C. elegans* Arp2/3 complex in cell migration during ventral enclosure. *J. Cell. Sci.* **116**, 1505-1518.
Shakir, M. A., Gill, J. S. and Lundquist, E. A. (2006). Interactions of UNC-34 Enabled with Rac GTPases and the NIK kinase MIG-15 in *Caenorhabditis elegans* axon pathfinding and neuronal migration. *Genetics* **172**, 893-913.
Shi, Y., Alin, K. and Goff, S. P. (1995). Abl-interactor-1, a novel SH3 protein binding to the carboxy-terminal portion of the Abl protein, suppresses v-Abl transforming activity. *Genes Dev.* **9**, 2583-2597.
So, C. W., So, C. K., Cheung, N., Chew, S. L., Sham, M. H. and Chan, L. C. (2000). The interaction between EEN and *abi-1*, two MLL fusion partners, and Synaptojanin and Dynamin: implications for leukaemogenesis. *Leukemia* **14**, 594-601.
Soto, M. C., Qadota, H., Kasuya, K., Inoue, M., Tsuboi, D., Mello, C. C. and Kaibuchi, K. (2002). The GEX-2 and GEX-3 proteins are required for tissue morphogenesis and cell migrations in *C. elegans*. *Genes Dev.* **16**, 620-632.
Stradal, T., Kranewitter, W., Winder, S. J. and Gimona, M. (1998). CH domains revisited. *FEBS Lett.* **431**, 134-137.
Stradal, T., Courtney, K. D., Rottner, K., Hahne, P., Small, J. V. and Pendergast, A. M. (2001). The Abl interactor proteins localize to sites of actin polymerization at the tips of lamellipodia and filopodia. *Curr. Biol.* **11**, 891-895.
Stradal, T. E., Rottner, K., Disanza, A., Confalonieri, S., Innocenti, M. and Scita, G. (2004). Regulation of actin dynamics by WASP and WAVE family proteins. *Trends Cell Biol.* **14**, 303-311.
Stringham, E. G., Dixon, D. K., Jones, D. and Candido, E. P. (1992). Temporal and spatial expression patterns of the small heat shock (hsp16) genes in transgenic *Caenorhabditis elegans*. *Mol. Biol. Cell* **3**, 221-233.
Stringham, E., Pujol, N., Vandekerckhove, J. and Bogaert, T. (2002). *unc-53* controls longitudinal migration in *C. elegans*. *Development* **129**, 3367-3379.
Stroschein-Stevenson, S. L., Foley, E., O'Farrell, P. H. and Johnson, A. D. (2006). Identification of *Drosophila* gene products required for phagocytosis of *Candida Albicans*. *PLoS Biol.* **4**, e4.
Takenawa, T. and Suetsugu, S. (2007). The WASP-WAVE protein network: connecting the membrane to the cytoskeleton. *Nat. Rev. Mol. Cell. Biol.* **8**, 37-48.
Tani, K., Sato, S., Sukezane, T., Kojima, H., Hirose, H., Hanafusa, H. and Shishido, T. (2003). Abl interactor 1 promotes tyrosine 296 phosphorylation of mammalian Enabled (Mena) by c-Abl kinase. *J. Biol. Chem.* **278**, 21685-21692.
Tanos, B. E. and Pendergast, A. M. (2007). Abi-1 forms an epidermal growth factor-inducible complex with Cbl: role in receptor endocytosis. *Cell. Signal.* **19**, 1602-1609.
Volkmann, N., Amann, K. J., Stoilova-McPhie, S., Egile, C., Winter, D. C., Hazelwood, L., Heuser, J. E., Li, R., Pollard, T. D. and Hanein, D. (2001). Structure of Arp2/3 complex in its activated state and in actin filament branch junctions. *Science* **293**, 2456-2459.
Wadsworth, W. G. (2002). Moving around in a worm: Netrin UNC-6 and circumferential axon guidance in *C. elegans*. *Trends Neurosci.* **25**, 423-429.
Watari-Goshima, N., Ogura, K., Wolf, F. W., Goshima, Y. and Garriga, G. (2007). *C. elegans* VAB-8 and UNC-73 regulate the SAX-3 receptor to direct cell and growth-cone migrations. *Nat. Neurosci.* **10**, 169-176.
Withee, J., Galligan, B., Hawkins, N. and Garriga, G. (2004). *Caenorhabditis elegans* WASP and Ena/VASP proteins play compensatory roles in morphogenesis and neuronal cell migration. *Genetics* **167**, 1165-1176.
Yu, T. W., Hao, J. C., Lim, W., Tessier-Lavigne, M. and Bargmann, C. I. (2002). Shared receptors in axon guidance: SAX-3/Robo signals via UNC-34/Enabled and a Netrin-independent UNC-40/DCC function. *Nat. Neurosci.* **5**, 1147-1154.
Zallen, J. A., Yi, B. A. and Bargmann, C. I. (1998). The conserved immunoglobulin superfamily member SAX-3/Robo directs multiple aspects of axon guidance in *C. elegans*. *Cell* **92**, 217-227.
Zhao, Z., Fang, L., Chen, N., Johnsen, R. C., Stein, L. and Baillie, D. L. (2005). Distinct regulatory elements mediate similar expression patterns in the excretory cell of *Caenorhabditis elegans*. *J. Biol. Chem.* **280**, 38787-38794.